# A FLAGELLUM BASED STUDY OF SEMICONDUCTOR NANOFABRICATION THROUGH MAGNETOTAXIS

ISAAC MACWAN, ZIHE ZHAO, OMAR SOBH AND PRABIR PATRA

*Abstract*— **Magnetospirillum *magneticum* (AMB-1), which belong to alpha-protobacterium are gram-negative, single-celled prokaryotic organisms consisting of a lash-like cellular appendage called flagella. These filamentous structures are made up of a protein called flagellin that in turn consist of four sub-domains, two inner domains (D0, D1) made up of alpha-helices and two outer domains (D2, D3) made up of beta sheets. It is wrapped in a helical fashion around the longitudinal filament with the outermost sub-domain (D3) exposed to the surrounding environment. This study focuses on the interaction of the D3 with semiconducting as well as metallic single-walled carbon nanotubes (m-SWNT) and in turn presents the interactive forces between the SWNT and D3 from the perspective of size and type of SWNT. It is found that the SWNT interacts the most with glycine and threonine residues of flagellin both electrostatically as well as through van der waals. Further, the viability of magnetotactic bacteria Magnetospirillum *magneticum* (AMB-1) in the presence of SWNT is experimentally investigated and it is found that magnetotaxis in AMB-1 is preserved without any toxic effects due to SWNT. It is proposed that AMB-1 can be used as an efficient carrier of carbon nanotubes through its flagellum for semiconductor nanofabrication tasks.**

## I. INTRODUCTION

One of the important aspects of the nano-bio-fabrication is the precise control of the atomic scale assembly so as to govern the process by which organic and inorganic molecules are bound with each other. This requires a thorough insight into the interactive forces that lie behind such an assembly. In semiconductor manufacturing, such an approach is called a bottom-up strategy in contrast to a top-down approach, where repeated steps of deposition and etching creates the required components.

Magnetospirillum *magneticum* (AMB-1) is one of the magnetotactic bacterial species that was first discovered in the year 1991 [1], [2]. Even before AMB-1 was isolated, the then known species called Aquaspirillum *magnetotacticum* (later on Magnetospirillum *magnetotacticum* - MS-1) was already known to exhibit magnetotaxis (ability to displace through magnetic field) whereby the bacterium could align itself to the earth's magnetic field and also to the locally generated magnetic field [3], [4]. It was found that such a response was due to the iron rich superparamagnetic nanoparticles embedded inside the bacterial cell, a detailed characterization of which revealed single domain iron oxide crystals having species specific size and distributions [5], [6] [7], [8]. AMB-1 is known to have a polar flagellum configuration where each flagellum is located at the proximal and distal ends of the spiral cell [9]. This is very similar to the flagella configuration found in another Magnetospirillum species called Magnetospirillum *gryphiswaldense* [10]. The swimming characteristics of the AMB-1 cells have also been thoroughly investigated from the viewpoint of speed, size of the cell and toxic chemicals in the environment, both for aerobic and anaerobic cultures [11]. Also, the flagellar motor of AMB-1 is comparable to E. Coli with same polar configuration and hence it has the same characteristics as that of an E. Coli flagellar motor such as 100Hz frequency corresponding to a speed of approximately 49μm/s and nearly 4.5 pN of thrust force [12]. Such flagellar filaments can have lengths in the range of 0.9 to 3.8 μm and a diameter from 12 to 19.5nm [13].

A single unit cell of the flagellum is made up of protein flagellin and in an 11-helix dual turn of a single flagellum, there are 11 such protofilaments [14]. The size of each flagellin is 140 Å in length and 110 Å in width and is in a position perpendicular to the filament axis [15]. The N-terminal is exposed to the environment, whereas the C-terminal is exposed to the central channel ~20Å in diameter [15]. There are two major conformations of flagellin, L (Left) -type and R (Right) -type. During the normal bacterial motion called 'run', the flagellin conformation is L-type. However, when the bacteria encounters an unfavourable condition such as a toxic environment, increased oxygen levels or increased temperature, it often does a 'tumble' which is when it abruptly changes its direction of motion. During such an event, the usual anti-clockwise motion of the flagellum is suddenly converted to clockwise and this sudden abruption in the flagellar motor twists the flagellin monomers, which looses their co-ordination and hence their conformation to R-type. The molecular structure of both L-type and R-type flagellin monomers is already known from electron cryomicroscopy [14], [15] and is also available from protein data bank. Some of the investigations in the past based on molecular dynamics (MD) simulations on the bacterial flagellum involved the motion of a rotating bacterial flagellum [16], the domain movement of the cap protein HAP2 from the viewpoint of flagellum growth [17] and the transportation of flagellin through the central channel for flagellar assembly [18]. So far there is very little information available on the conformation of flagellin in the

I. G. Macwan is with the Department of Computer Science & Engineering, University of Bridgeport, Bridgeport, CT 06604 USA (e-mail: imacwan@my.bridgeport.edu).

Z. Zhao is with the Department of Computer Science, University of Bridgeport, Bridgeport, CT 06604 USA (e-mail: zihezhao@my.bridgeport.edu).

O. T. Sobh is with the Department of Biology, University of Pennsylvania, Philadelphia, PA 19104 USA (osobh@sas.upenn.edu).

P. K. Patra is with the Department of Mechanical Engineering and Biomedical Engineering, University of Bridgeport, Bridgeport, CT 06604 USA, (Phone: 203-576-4165; e-mail: ppatra@bridgeport.edu).

978-1-4244-7929-0/14/$26.00 ©2014 IEEE

presence of SWNT and their interactions. The purpose of this work is to gain insights on the interactive behavior of flagellin with metallic as well as semiconducting SWNT from the perspective of functionalizing the flagellum of live AMB-1 cells so as to use these magnetically controllable species in nanofabrication tasks. Molecular dynamics is used to study such interactive forces and it is found that residues GLY and THR are the most favorable ones that are adsorbed on the m-SWNT in the first 5ns time span (keeping the SWNT at a distance of 15Å initially). The energy graphs and the trajectory information indicate that SWNT interacts with the flagellin from as far as 50Å away and van der waals forces are dominant once the distance reduces to 5Å and below. It is also found that semiconducting (5,15) SWNT takes twice as much time to get adsorbed as compared to metallic (12,12) SWNT. The experimental results further show that AMB-1 cells can be cultivated in the presence of SWNT without any significant effect on the size or magnetotactic behavior of the cells. Magnetic experiments indicated that AMB-1 can preserve magnetotaxis in the presence of SWNT and can be utilized as SWNT transporters without any toxicological effect.

## II. Materials and Methods

Magnetospirillum *magneticum* (AMB-1) (ATCC - 700264) was purchased and cultivated in-house using the MSGM (magnetospirillum growth medium) protocol given by ATCC. The culture media per 1L of distilled water included: 10ml Wolfe's vitamin solution, 5ml Wolfe's mineral solution, 2ml 0.01M ferric quinate, 0.45ml 0.1% resazurin, 0.68g $KH_2PO_4$, 0.12g $NaNO_3$, 0.035g ascorbic acid, 0.37g tartaric acid, 0.37g succinic acid, 0.05g sodium acetate and 1.3g agar (for semi-solid media). After adding the chemicals, the media was checked for the pH of 6.75 and if needed, 0.5M NaoH and HCL is used to set the pH. The media is then autoclaved at 121$^{o}$ C for 15 minutes and about 1ml of inoculum is injected to a 10ml screw-cap test tube aseptically. The carbon nanotubes for the magnetic experiments were purchased from cheaptubes Inc.

Molecular dynamics simulations were prepared and analyzed using VMD (visual molecular dynamics) [19] and were carried out using NAMD [20]. R-type flagellin filament pdb file (code 1UCU [15]) was obtained from protein data bank and an inbuilt nanotube builder plugin was used to create SWNTs of metallic (12,12) as well semiconducting (5,15) nature with lengths of 1.2nm and 5nm. Domain D3 (97 residues) was isolated from the R-type flagellin monomer (fig. 1A) for simulation purposes in one set of simulations. The other set consisted of the entire flagellin monomer (494 residues). All simulations used the CHARMM force field [21] along with TIP3 water model [22] with a neutralizing salt concentration of NaCl for effective polarization of water molecules.

In each simulation, temperature was maintained at 300K by Langevin thermostat and pressure of 1atm was maintained through Nose-Hoover Langevin-piston barostat with a period of 100ps and a decay rate of 50ps; periodic boundary conditions were assumed. Multiple time stepping was employed using an integration timestep of 2fs, with short-range forces evaluated every time step and long range electrostatic forces evaluated every two timesteps. Short range forces were smoothed with a cutoff between 10 and 12 Å, while long range electrostatic forces were calculated using the particle-mesh Ewald algorithm. A salt strength just enough to neutralize the charge of the system was assumed. All-atom simulations of both the interactions between D3 and SWNT and between R-type flagellin monomer and SWNT were performed in a periodic water box. The analysis plugins for root mean square deviation (RMSD) and NAMD energy were utilized to further analyze the nature of interactive forces and associated energies.

Dell Studio XPS 9100 system with 8-core Intel i7 CPU and 16-core CUDA acceleration capability was utilized to perform the MD simulations. Optical microscopy was utilized to perform the magnetic experiments involving straight as well as coiled conductors.

## III. Results and Discussion

### A. Simulation of (6,6) 1.2nm long SWNT and flagellin monomer

Fig. 1A shows the structure of the flagellin monomer with the four domains. Domains D0 and D1 are predominantly made up of alpha helices and domains D2 and D3 are predominantly extended beta sheets.

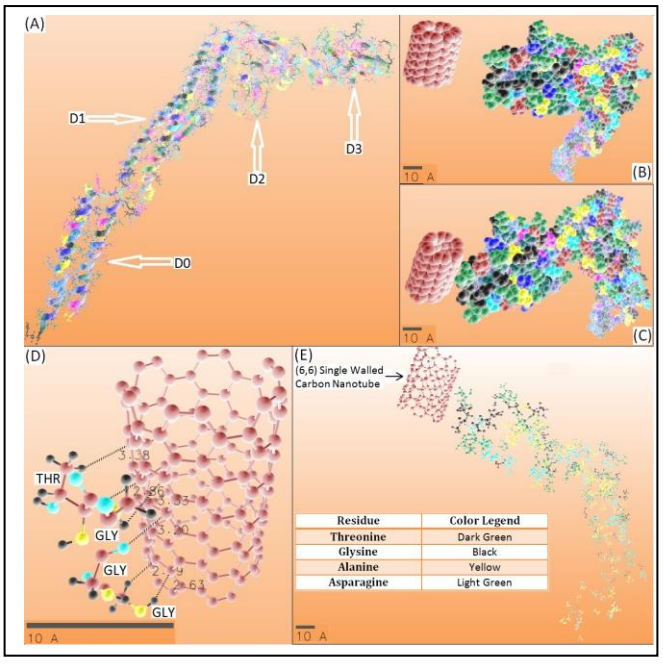


Figure 1. (A) Flagellin monomer showing the four domains (B), (C) m-SWNT simulations showing the state of flagellin monomer and SWNT before and at the end of a 10ns simulation run (D) GLY and THR having the most favorable interaction with the m-SWNT as displayed by the distances in the range of wan der waal binding (3.38Å, 2.86Å, 3.33Å, 3.20Å, 2.49Å and 2.63Å) (E) Four type of residues (Threonine, Glysine, Alanine and Asparagine) having the most significant effect on the binding kinetics in flagellin

Fig. 1B and 1C show the initial and final states of the flagellin monomer relative to a m-SWNT at the end of 11ns

simulation run. As seen from fig. 1D, three glycine (GLY) residues and one threonine (THR) residue are all involved in binding the m-SWNT. GLY by nature is aliphatic, non-polar and THR is polar, uncharged. Hence, as seen from fig. 1D, GLY and m-SWNT interactions were the most favorable with distances well in the range of strong wan der waal forces (2.63Å, 2.69Å and 2.86Å). THR also exhibited favorable interactions with the m-SWNT at a distance of 3.38Å. Fig. 1E exhibits the different residues that have been observed as binding with the m-SWNT with maximum binding energies.

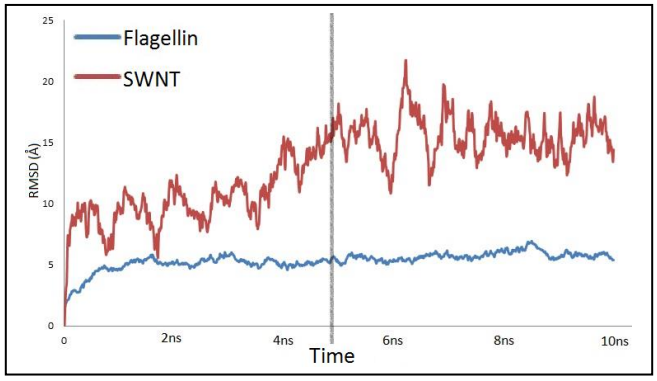


Figure 2. RMSD for flagellin monomer and m-SWNT

Fig. 2 shows the RMSD graph of both flagellin and SWNT displaying an interesting trend where the protein started adsorbing on the SWNT surface in as quickly as 5ns of time period (black shaded line) indicated by a steady RMSD profile of SWNT (red) after a jump from an average of 8Å to an average of 15Å displacement from the initial position. 15Å was the initial distance between flagellin and SWNT before the start of the simulation and hence consecutive smaller peaks in the RMSD after 7ns indicates a stable adsorption.

### *B. Simulation of (12,12) 5nm long SWNT and D3 domain of flagellin*

Fig. 3A shows the interaction of domain D3 with a (12,12) 5nm long m-SWNT initially ~50Å away and at the end of 10ns run, ~43.8Å away. Comparison with D3 in the absence of SWNT revealed that the change in displacement of D3 to ~14Å as displayed by the RMSD (fig. 3B) in case of a remote SWNT is due to the electrostatic interactions between the remote SWNT and D3. These electrostatic interactions in the presence and absence of SWNT (fig. 3C and 3D) revealed an energy difference of ~100kcal/mol. This shows how the outer domain D3 of the flagellin monomer starts interacting with a m-SWNT from as far as ~44Å. These results further imply that binding of SWNT and flagellin would be guided without any special functionalization chemistry.

### *C. Simulation of (5,15) 5nm SWNT and D3 domain of flagellin*

Fig. 4A shows the interaction of semiconducting (5,15) SWNT with D3 domain. It is found that the semiconducting

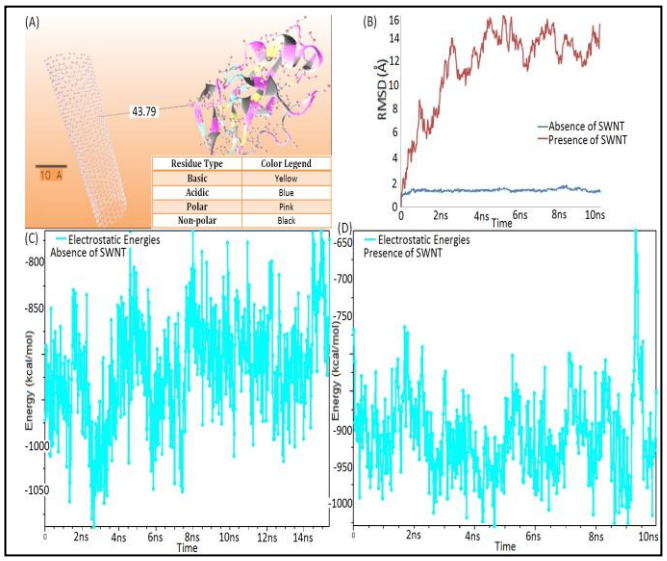


Figure 3. (A) Interaction of (12,12) m-SWNT with D3 of flagellin (B) RMSD for flagellin in the presence (red) and absence (blue) of SWNT (C), (D) Electrostatic energy profile of D3 in the absence and presence of SWNT

SWNT takes twice as long to approach a stable state when it interacts with D3 (fig. 4C). When compared to the m-SWNT case having the same length of 5nm, the electrostatic energy is also not stable (fig. 4B) and hence it suggested that semiconducting SWNT would take twice as long to form a stable bond with D3 and hence the flagellin monomer. The RMSD analysis of D3 and semiconducting SWNT revealed this peculiar behavior of interaction kinetics.

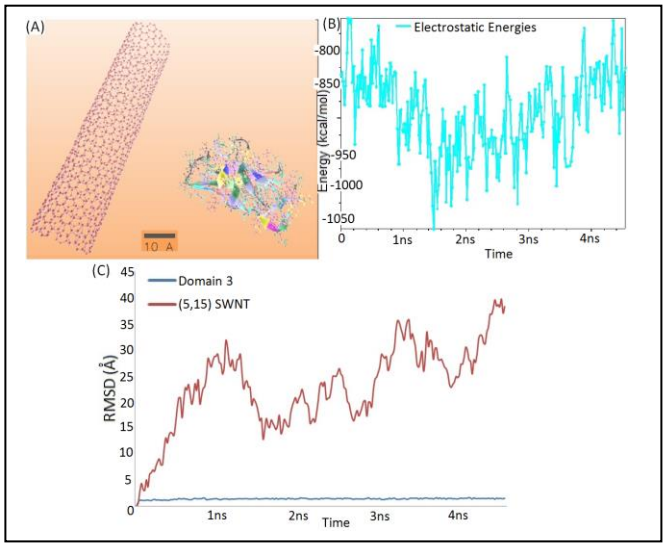


Figure 4. (A) Interaction of semiconducting (5,15) SWNT with D3 domain of flagellin (B) Electrostatic energy graph showing an unstable binding for the first 5ns (where m-SWNT was already stabilized) (C) RMSD plots of D3 and SWNT showing an unstable binding for the first 5ns.

Experimental analysis of AMB-1 cells in the presence of SWNT revealed that AMB-1 can survive in the presence of SWNT and magnetotaxis is conserved. The cell response, size and shape are unaltered indicating that the toxic effects of SWNT are not of a concern for AMB-1 cultivation. Thus,

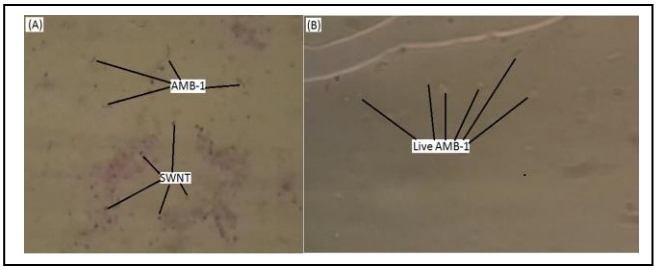


Figure 5. (A) Optical image showing heat fixed AMB-1 cells along with SWNT bundles (as nanotubes are hydrophobic) (B) Live AMB-1 cells near the edge of the suspended water drop under the effect of magnetic field through a permanent magnet near the microscope stage.

AMB-1 can be utilized for effective transport of SWNT as anticipated through the MD simulations. Fig. 5 shows the optical images of AMB-1 cells in the presence of SWNT.

## IV. Conclusion

Molecular dynamics simulations are performed both on the entire flagellin monomer and its isolated domain D3 in the presence of both metallic as well as semiconducting SWNT. NAMD is utilized to perform simulation runs for 10ns and it is found that SWNT most favorably interacts with GLY as well as THR residues. Furthermore, m-SWNT stabilizes twice as fast as semiconducting SWNT and this is portrayed from the RMSD as well as electrostatic energy profiles of the two types of SWNTs. In comparison with the D3 domain alone, the displacement of D3 in the presence of SWNT is mainly due to the electrostatic interactions even though the SWNT is remotely located. The use of these interactions gives useful insights into functionalizing the flagellum of live AMB-1 cells with SWNT, thereby providing precise transport of SWNT through magnetotaxis that is solely governed by AMB-1. Magnetic analysis of AMB-1 in the presence of SWNT suggests a favorable environment where AMB-1 can be functionalized with SWNT without any specialized chemical functionalization.

## Acknowledgment

We thank Dr. Jinnque Rho from the department of Biology at the University of Bridgeport for his helpful insights and guidance towards bacterial cultivation.

## References

[1] T. Matsunaga, T. Sakaguchi, and F. Tadokoro, "Magnetite formation by a magnetic bacterium capable of growing aerobically.," Applied Microbiology and Biotechnology, vol. 35, pp. 651-655, 1991.

[2] R. Kawaguchi, J. G. Burgess, and T. Matsunaga, "Phylogeny and 16s rRNA sequence of Magnetospirillum sp. AMB-1, an aerobic magnetic bacterium.," Nucleic Acids, vol. 20, pp. 1140, 1992.

[3] R. Blakemore, "Magnetotactic bacteria," Science, vol. 190, pp. 377-379, 1975.

[4] B. M. Moskowitz, R. B. Frankel, P. J. Flanders, R. Blakemore, and B. B. Schwartz, "Magnetic properties of magnetotactic bacteria," Magnetism and Magnetic Materials, vol. 73, pp. 273-288, 1988.

[5] R. E. Dunin-Borkowski, M. R. McCartney, R. B. Frankel, D. A. Bazylinski, M. Posfai, and P. R. Buseck, "Magnetic microstructure of magnetotactic bacteria by electron holography," Science, vol. 282, pp. 1868-1870, 1998.

[6] D. A. Bazylinski and R. B. Frankel, "Magnetosome formation in prokaryotes," Nature Reviews Microbiology, vol. 2, pp. 217-230, 2004.

[7] R. B. Proksch, T. E. Schaffer, B. M. Moskowitz, E. D. Dahlberg, D. A. Bazylinski, and R. B. Frankel, "Magnetic force microscopy of the submicron magnetic assembly in a magnetotactic bacterium.," Applied Physics Letters, vol. 66, pp. 2582-2584, 1995.

[8] D. Yamamoto, A. Taoka, T. Uchihashi, H. Sasaki, H. Watanabe, T. Ando, and Y. Fukumori, "Visualization and structural analysis of the bacterial magnetic organelle magnetosome using atomic force microscopy," Proceedings of the National Academy of Sciences of the United States of America, vol. 107, pp. 9382-9387, 2010.

[9] H. Choi, K.-i. Koo, S. Park, M.-J. Jeong, G. Kim, J. Park, J.-M. Lim, W.-J. Chung, L. Seung-Hwan, S. Jin, Y.-S. Lee, T. H. Park, J. Y. Yoo, and D.-i. Dan Cho, "Improvement of bacterial tethering using both physical and chemical surface modification for flagella spin actuators," Sensors and Actuatros B: Chemical, vol. 123, pp. 269-276, 2007.

[10] D. Schultheiss, M. Kube, and D. Schuler, "Inactivation of the flagellin gene flaA in magnetospirillum gryphiswaldense results in nonmagnetotactic mutants lacking flagellar filaments," Applied and Environmental Microbiology, vol. 70, pp. 3624-3631, 2004.

[11] S. Seong and T. H. Park, "Swimming characterisitics of magnetic bacterium Magnetoprillum sp. AMB-1, and implications as toxicity measurement," Biotechnology and Bioengineering, vol. 76, pp. 11-16, 2001.

[12] H. C. Berg and L. Turner, "Torque generated by the flagellar motor of Escherichia Coli," Journal of Biophysics, vol. 65, pp. 2201-2216, 1993.

[13] K. T. Silva, F. Abreu, F. P. Almeida, C. N. Keim, M. Farina, and U. Lins, "Flagellar apparatus of south-seeking many-celled magnetotactic prokaryotes," Microscopy research and technique, vol. 70, pp. 10-17, 2007.

[14] S. Maki-Yonekura, K. Yonekura, and K. Namba, "Conformational change of flagellin for polymorphic supercoiling of the flagellar filament," Nature Structural and Molecular Biology, vol. 17, pp. 417-423, 2010.

[15] K. Yonekura, S. Maki-Yonekura, and K. Namba, "Complete atomic model of the bacterial flagellar filament by electron cryomicroscopy," Nature, vol. 7, pp. 643-650, 2003.

[16] A. Arkhipov, P. L. Freddolino, K. Imada, K. Namba, and K. Schulten, "Coarse-grained molecular dynamics simulations of a rotating bacterial flagellum," Biophysical Journal, vol. 91, pp. 4589-4597, 2006.

[17] S. Maki-Yonekura, K. Yonekura, and K. Namba, "Domain movements of HAP2 in the cap-filament complex formation and growth process of the bacterial flagellum," Proceedings of the National Academy of Sciences of the United States of America, vol. 100, pp. 15528-15533, 2003.

[18] D. E. Tanner, W. Ma, Z. Chen, and K. Schulten, "Theoretical and computational investigation of flagellin translocation and bacterial flagellum growth," Biophysical Journal, vol. 100, pp. 2548-2556, 2011.

[19] W. Humphrey, A. Dalke, and K. Schulten, "VMD: Visual molecular dynamics," Journal of Molecular Graphics, vol. 14, pp. 33-38, 1996.

[20] J. C. Phillips, R. Braun, W. Wang, J. Gumbart, E. Tajkhorshid, E. Villa, C. Chipot, R. D. Skeel, L. Kale, and K. Schulten, "Scalable molecular dynamics with NAMD," Journal of Computational Chemistry, vol. 26, pp. 1781-1802, 2005.

[21] A. D. Mackerell, D. Bashford, R. L. Dunbrack Jr., J. D. Evanseck, M. J. Field, S. Fischer, J. Gao, H. Guo, S. Ha, D. Joseph-McCarthy, L. Kuchnir, K. Kuczera, F. T. K. Lau, C. Mattos, S. Michnick, T. Ngo, D. T. Nguyen, B. Prodhom, W. E. Reiher, B. Roux, M. Schlenkrich, J. C. Smith, R. Stote, J. Straub, M. Watanabe, J. Wiorkiewicz-Kuczera, D. Yin, and M. Karplus, "All-atom empirical potential for molecular modeling and dynamics studies of proteins," Journal of Physical Chemistry B., vol. 102, pp. 3586-3616, 1998.

[22] W. L. Jorgensen, J. Chandrasekhar, J. D. Madura, R. W. Impey, and M. L. Klein, "Comparison of simple potential functions for simulating liquid water," Journal of Chemical Physics, vol. 79, pp. 926, 1983.